Journal of Applied Polymer Science

Main events occurring in styrene microemulsion polymerization

J. Esteban López-Aguilar,[1] René O. Vargas,[2] Carlos E. Escobar-Toledo,[1] Eduardo Mendizábal,[3] Jorge. E. Puig,[3] Francisco López-Serrano[1]

[1]Facultad de Química, Departamento de Ingeniería Química, Universidad Nacional Autónoma de México 04510, México
[2]SEPI ESIME Azcapotzalco, Instituto Politécnico Nacional, Avenida de las Granjas No. 682, Colonia Santa Catarina, Delegación Azcapotzalco, México, Distrito Federal 02250, Mexico
[3]CUCEI, Departamentos de Química e Ingeniería Química, Universidad de Guadalajara, Jalisco 44430, México
Correspondence to: F. López-Serrano (E-mail: lopezserrano@unam.mx)

ABSTRACT: A previously presented model with four states (conversion, active and inactive particles and micelles) is further tested with conversion versus time experimental data at 50, 60, and 70°C, to recognize the main events occurring in styrene microemulsion polymerization. The S-shaped conversion–with no overprediction- and the bell-shaped active particles number concentration–evidencing diffusive effects at late stages–versus time data, are well described by the proposed model. It was found that: (i) transfer of monomer and surfactant from micelles to particles occurs, (ii) the capture of radicals by micelles is the only cause of particle nucleation, (iii) the rate coefficient of radical-entry-to-micelles is much smaller than that of exit-from-particles, and (iv) no coagulation between particles was detected. The Arrhenius dependency on temperature of the kinetic rate parameters is also reported. © 2014 Wiley Periodicals, Inc. J. Appl. Polym. Sci. **2015**, *132*, 41720.

KEYWORDS: emulsion polymerization; kinetics; micelles; nanoparticles; theory and modeling

Received 29 August 2014; accepted 31 October 2014
DOI: 10.1002/app.41720

INTRODUCTION

Microemulsion polymerization (MEP) is a process in which several physical and chemical phenomena occur, such as phase equilibrium and complex reaction interfacial schemes. Due to these facts, MEP modeling is a case study in chemical engineering, presenting a challenge in parameter estimation and model assessment. There are important controversies in understanding this subject, which have been dealt with previously. Next, the most controversial mechanistic aspects are listed to put the problem into perspective.

Even for polymers whose glass transition temperature (T_g; K) is well below the reaction temperature (T), most of the reactions do not reach complete conversion, likely caused by diffusive (vitreous) effects, that have scarcely been treated.[1,2] Evidence of the existence of these effects has been detected by López-Serrano *et al.*,[3,4] and explained with a dramatic drop in the propagation rate constant $k_p(x)$ versus conversion curves at late reaction stages.

The steady state radical generation has always been considered for initiator decomposition.[1–13] Radical entry to particles involves the entrance of primary/oligomeric radicals to active and inactive particles. Here, differing proposals have dealt with this event by first[3,4] and second order mechanisms.[1,2,5–13] Notably, the majority of the studies concluded that no radical entry to particles occurs.[3,4,7–11,13] In contrast, Guo *et al.* and Mendizábal *et al.* proposed that this radical-entry to particles does exist,[1,2,5,6] and that its rate coefficient is considerably larger than that for radical entry to micelles.

Two approaches have been adopted for the coagulation mechanism: (i) the proposal by Chern and Tang with a dimensionless factor in front of the particle generation mechanism.[13] This attempt hinders particle generation and was assumed to be effective in the linear-N_1 prediction and (ii) the one by López-Serrano *et al.*, considering interactions between active (N_1) and inactive (N_0) particles in the reaction mixture,[3,4] which resulted non-existent for the systems studied.

Particle diameter prediction seems relatively accurate in order of magnitude, since experiments provide particles of about 10 nm in size.[1–4,7–10,13] In the majority of MEP modeling studies, the quantities commonly studied are the monomer conversion (x) and the active particle concentration (N_1). Here, the most outstanding controversies arise, for which most of the studies (i) overpredicted the conversion versus time data at late reaction stages, and (ii) predicted a linear evolution of the active particle concentration (N_1).[1,2,5–13] It is worth noting that López-Serrano *et al.* predicted (i) conversion versus time trends perfectly,[3,4]

and (ii) the non-linear bell-shaped behavior of the active particle concentration N_1, reported experimentally as a key identifying feature to MEP kinetics amongst other multiphase polymerization techniques.[3,4,11,12] These accurate predictions were achieved by considering a monomer and surfactant transport from micelles to particle mechanism as an approximation for the interaction between the monomer-swollen micelles and the active particles. This mechanism, elsewhere considered,[3,4] plays the role of an extra factor diminishing the number of particles, along with micellar nucleation.

The 0-1 system assumption has been used in most of the modeling exercises.[1–13] Nevertheless, this assumption has only been validated through an integro-differential (ID) approach, implemented by López-Serrano *et al.*[3,4,14]

In the polymer reaction engineering context, even for simple models, many parameters that represent the mechanistic events appear. Usually experimental data is scarce, and to overcome this difficulty, the ID approach has been proven to yield additional information contained in the measurement's derivatives.[3,4,14–18]

Despite the controversies outlined above,[19] not many MEP kinetic and modeling studies have been conducted lately. Moreover, modifications and new techniques based on MEP have emerged in recent years for complex polymeric particle production at the nano-scale,[20–23] such as differential MEP[20,21]; and more recently, reversible addition-fragmentation chain transfer polymerization via MEP,[22,23] just to mention a few. Hence, further research is required in resolving modeling controversies and MEP applicability; and to modify an existing process or to design a new one, for which the mechanisms knowledge is fundamental.

Here, a step is presented to contribute to the understanding of this intriguing MEP process. Thus, the temperature dependence and a parameter sensitivity analysis are assessed with a previously presented MEP kinetic model,[3,4] to test its applicability and to denote the main events occurring in this process. The procedure is applied to conversion versus time experimental data for styrene (STY) MEP, reported previously at 50, 60, and 70°C.[24]

THE MODEL

Our kinetic model is based on the following assumptions: (i) a 0-1 compartmentalized system (this will be validated later), (ii) the monomer concentration in the particles is given by the partition function proposed by Vries *et al.*,[11] (iii) the initial micelles number density can be measured or estimated,[3,4,25,26] (iv) the radical-entry to particles (ρ), to micelles (ρ_m) and radical-exit (k) from particle rates are described by first-order mechanisms with respect to their concentration, (v) pseudo-steady state for the concentration of the radicals in aqueous phase applies, (vi) the decrease in the number density of micelles (emulating the monomer and surfactant transport) is approximated by a coagulation mechanism (k_o) between micelles and active particles mechanism, (vii) particle coagulation rate coefficient (k_c) between particles (active-active, active-inactive and inactive-inactive) can take place; these last two events are described by second-order mechanisms, (viii) homogeneous nucleation is not considered due to the negligible monomer water solubility.[11]

The initial condition problem, resulting from the species balance and the assumptions stated above, is depicted by the following five equation-set:

$$\frac{dx}{dt} = B(1-x)^b N_1; \quad B = \frac{k_p C_{m0}}{M_0 N_{Av}}; \quad x(0) = 0 \tag{1}$$

$$\frac{dN_m}{dt} = -\rho_m N_m - k_o N_1 N_m; \quad N_m(0) = N_{m0} \tag{2}$$

$$\frac{dN_1}{dt} = \rho(N_0 - N_1) - kN_1 + \rho_m N_m - 2k_c N_1^2; \quad N_1(0) = 0 \tag{3}$$

$$\frac{dN_0}{dt} = \rho(N_1 - N_0) + kN_1 + k_c\left(N_1^2 - N_1 N_0 - N_0^2\right); \quad N_0(0) = 0 \tag{4}$$

$$\frac{dR^*}{dt} = 2fk_d I N_{Av} + kN_1 - \rho(N_1 + N_0) - \rho_m N_m - \frac{2k_t R^{*2}}{N_{Av}}; \quad R^*(0) = 0. \tag{5}$$

Here, x is the conversion, t is the reaction time (s), k_p and k_t are the propagation and termination rate constants (L mol^{-1} s^{-1}), C_{m0} is the initial monomer concentration in the particles (mol L^{-1}), M_0 is the initial monomer concentration in the reactor (mol L^{-1}), N_{Av} is the Avogadro number, and N_1 and N_0 are the active and inactive particle concentrations (L^{-1}), respectively. The micelles concentration is N_m (L^{-1}) and N_{m0} is its initial concentration, and b is a parameter characterizing the monomer partition.[11] The model considers only micellar nucleation, ρ_m (s^{-1}); chain growth termination is by chain transfer to monomer and further desorption from particles, k (s^{-1}); there is radical entry to particles, ρ (s^{-1}); swollen micelles can transfer monomer and surfactant to active particles, which is approximated by k_o (L mol^{-1} s^{-1}); and the coagulation between particles is considered, k_c (L mol^{-1} s^{-1}).[3,4] The radical concentration in the aqueous phase is R^* (L^{-1}); thus, f (dimensionless), k_d (s^{-1}) and I (mol L^{-1}) are the initiator efficiency, its decomposition rate constant and concentration, respectively. The values used in the model are listed in Table I. The initial micelle concentration was obtained by the following equation[31]:

$$N_{m0} = (S - \mathrm{CMC})\frac{N_{\mathrm{av}}}{n_{\mathrm{agg}}}, \tag{6}$$

here, S is the concentration of emulsifier (mol L^{-1}), CMC is the critical micellar concentration (mol L^{-1}) and n_{agg} the emulsifier aggregation number (dimensionless).

The instantaneous number molecular mass (M_n) is calculated as the quotient of the propagation to the termination events, multiplied by the monomer's molecular mass as follows[32]:

$$M_n = \frac{k_p C_m}{k + k_p C_M C_m} M_m, \tag{7}$$

where M_m is the monomer molecular mass and C_M (dimensionless) is the transfer to monomer ratio $[k_p/k_{tr,M}]$, whereas the number-average molecular mass ($\bar{M}_n$) is obtained applying the Mean Value Theorem to eq. (7). Here, termination by radical desorption and chain transfer to monomer mechanisms are considered.

Table I. Model Parameters

Parameters	Value
b (–)[11]	1
k_p (L mol^{-1} s^{-1})[26]	$4.27\times10^{7}e^{-\frac{32.51}{R(kJ/molK)T}}$
k_t (L mol^{-1} s^{-1}) @ P=1.01325 bar[27]	$e^{17.14-1.873\times10^{-4}P-\frac{3748}{T}+\frac{0.202P}{T}}$
C_{m0} (mol L^{-1})[11]	1.67
S (mol L^{-1})[24]	0.3814
CMC (mol L^{-1})[28]	0.008
M_0 (mol L^{-1})[24]	0.5769
ρ_P (g L^{-1})[29]	1048
M_{we} (g mol^{-1})	288
M_m (g mol^{-1})	104
n_{ag} (–)[30]	64
a_s (Å^2)[30]	45
f	0.5
I_o (mol L^{-1})[24]	0.00025

The number of particles is given by the following mass balance:

$$N_T = \frac{xM_0M_m}{\rho_P\left[\frac{4}{3}\pi\left(\frac{D_p}{2}\right)^3\right]}, \quad (8)$$

the polymer density is ρ_p and the particle diameter can be estimated as:

$$D_p = \left(\frac{6}{\pi}\frac{xM_0M_m}{\rho_P N_T}\right)^{1/3}. \quad (9)$$

The initial conditions, in eq. set (1)–(5), are all known. A simple inspection yields that eqs. set (2)–(4) is coupled, being autonomous from eq. (1) and (4). Moreover, eqs. (1) and (5) are coupled with eqs. sets (2)–(4). At this stage, our problem consists of solving the above five-equation-set (x, N_0, N_1, N_m, R^*), involving five unknown parameters (ρ, ρ_m, k, k_c, k_o), with only conversion and particle diameter data.

THE INTEGRODIFFERENTIAL APPROACH: INFERRING AN ADDITIONAL MEASUREMENT

As mentioned above, given all the possible events occurring in MEP, even in a simple model, as the one presented in the previous section, many parameters appear. In our case, five parameters and only two measurements (x and N_T) are not enough to determine them all in a unique fashion.

The procedure to generate an additional, inferred, experimental measurement is explained elsewhere.[3] Here, a simplified version is given. Observing eq. (1), the lumped parameter B (s^{-1}) and parameter b are, in principle, constant and known. Therefore, if the conversion derivative is known, the trajectory of N_1 can be inferred ($\hat{N}_1$). To obtain the conversion-time-derivative, proceed as follows: First propose an empirical function that describes the experimental conversion data (y) to a predetermined precision; an alternative is to use splines.[33] Take the time-derivative of this function to yield dy/dt (Differential method).[34] The result is:

$$\hat{N}_1 = \frac{\frac{dy}{dt}}{B(1-y)^b}. \quad (10)$$

Therefore, the RHS of eq. (10) is known and $\hat{N}_1$ can be obtained. Now our problem consists of finding the five parameters (ρ, ρ_m, k, k_c, and k_o), given the known initial conditions in the eq.-set (1)–(5), now with three experimental measurements: (i) conversion-versus-time (x), (ii) the inferred concentration of active particles ($\hat{N}_1$) and (iii) data for N_0 (= N_T – $\hat{N}_1$); N_T is obtained from eq. (8). To solve this problem, a standard regression method is used (Integral method). A simple analysis of eq.-set (1)–(5) makes it possible to find that the additional inferred measurement imparts a high level of robustness to the solution, because it appears in the whole equation-set.

The diffusive effects can be accounted for by calculating the propagation rate k_p as a function of conversion as follows[3,4]:

$$k_p(x) = k_p\frac{\hat{N}_1}{N_1}, \quad (11)$$

where $k_p(x)$ is the value of k_p which accurately predicts N_1.

RESULTS AND DISCUSSION

Conversion

The experimental conversion-versus-time data for styrene MEP at 50, 60, and 70°C were taken from Chern and Wu.[24] Figure 1(a) compares the predictions of our model (thick lines) against experimental data (symbols) of conversion versus time, for the three temperatures. Here, it is evident that the model accurately describes the experimental trends. Conspicuously and contrary to other models,[1,2,5–13] our model does not overpredict the conversion-versus-time experimental results. It is worth mentioning that the Chern and Tang's model[13] is the one proposed previously,[7,10,11] with an added fitting factor called coagulation factor, F (dimensionless)[14] shown in Figure 1(a; thin lines) for comparison. In contrast to our model, and during the intermediate and final stages of the reaction, Chern and Tang's overpredicts the conversion-versus-time data for all the temperatures [Figure 1(a)], even when particle coagulation is considered.

Active Particle Concentration N_1

The evolution of active particle concentration (N_1) versus time is well described by our model [Figure 1(b)], yielding the bell-shaped curve depicted by the inferred data ($\hat{N}_1$). Again, this result contradicts hypotheses made earlier,[7,11,13] in which a linear N_1 behavior with time was assumed. Furthermore, these findings confirm the ones previously obtained.[3,4,14] For the lower temperatures, N_1 results slightly over-predict the inferred active particle concentration ($\hat{N}_1$) at late reaction stages. This could be related to diffusion limitation effects within the particles in the propagation step. This fact has been found for other systems, including soft ones in which the polymer T_g is considerably lower than the reaction temperature.[3,4] Figure 1(b) also shows the predictions made by Chern and Tang's model (thin lines).[13] The fitted particle coagulation factors were F = [0.027, 0.030, 0.018] for T = [50, 60, 70]°C, respectively. This model describes a linear dependency of the active particle

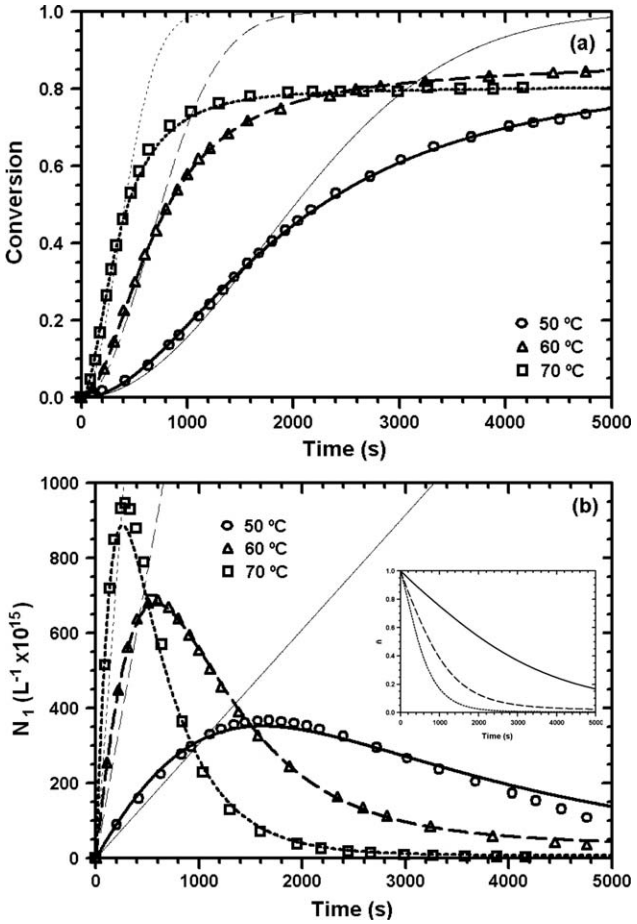

Figure 1. Styrene MEP at 50, 60, and 70 °C. (a) Conversion (x) and (b) Active particles number (N_1) against time data. Symbols correspond to experimental conversion[24] or inferred ($\hat{N}_1$) data. Thick lines depict model results, and thin lines correspond to Chern and Tang's model.[24] The inset shows the average number of radicals per particle $\tilde{n}$ ($=N_1/N_T$) time evolution as described by the proposed model.

concentration on time [thin lines in Figure 1(b)], in contrast to our inferred bell-shaped data. The reason for Chern and Tang's model over prediction is due to the fact that, although the active particles generation is a linear function with time, the coagulation factor only dampens this behavior, and this mechanism prevails along the reaction. However, our model (eq. (2)) takes into account the monomer and surfactant transfer by disappearing micelles with the term $k_o N_m N_1$, allowing the active particles decrease by means of the term $\rho_m N_m$ in eq. (3).

Besides, the assumption that a 0-1 system prevailed was validated, as shown in the inset of Figure 1(b), where the values of average radical number per particle $\tilde{n}$ ($=N_1/N_T$) never exceeds the value of one. A value of one is reached at the beginning of the reaction because all new particles are active. Inactive particles will start to appear when the fate of radicals exit prevails, preceded by transfer to monomer.

Diffusive Effects

Particular attention should be paid to the evolution of N_1. Figure 1(b) discloses a slight over-prediction with respect to the experimental/inferred values for N_1 at the end of the polymerization reaction, as pointed out previously. This fact appears enhanced at the lowest reaction temperature; here, we argue that this over-prediction is due to diffusive effects in the propagation step. As mentioned earlier, this phenomenon has already been found for other systems, even for polymers with a T_g lower than the reaction temperature.[3,4] The results obtained solving eq. (11) are shown in Figure 2. This figure depicts that the evolution of $k_p(x)$ versus conversion has a nearly constant behavior at early reaction stages, according to the assumption that k_p was constant; however, at the end of the reaction it drops out suddenly, indicating that in this part of the process, the reaction stops because the monomer cannot diffuse through the particle and react with the free radical attached to a polymer chain. This diffusive effect is more dramatic and begins earlier for lower reaction temperatures, clearly shown by the 50 and 60°C curves. Accordingly, when the reaction temperature is lower, the system is closer to the overall glass transition temperature, causing the medium to be more solid-like and preventing the species movement in the particles. One could believe that at a lower temperature the active particle number should be lower, presented in Figure 1(b), where at longer times for the lower temperature a higher active particle number is observed, even though these active radicals prevail in the particles—they are trapped in the polymer matrix (vitreous effect) and cannot polymerize. This is shown more clearly in Figure 2 (k_p vs. x), where the slowing down of k_p appears at lower conversions. As shown in the conversion against time curve [Figure 1(a)], there is an overlapping of the curves at 70 and 60°C, which is attributed to minor experimental errors; however, this is not reflected in the parameter trends estimations. For the 70°C curve, a similar behavior is observed, but an unexpected intersection with the 60°C curve occurs. This result seems to be due to the intersection of the corresponding conversion-versus-time trends [see Figure 1(a)] and to the fact that eq. (10) requires the smoothed conversion curves. Therefore, if experimental errors exist, they are reflected and propagated by this method, especially in the low-in-information zone.[15–18]

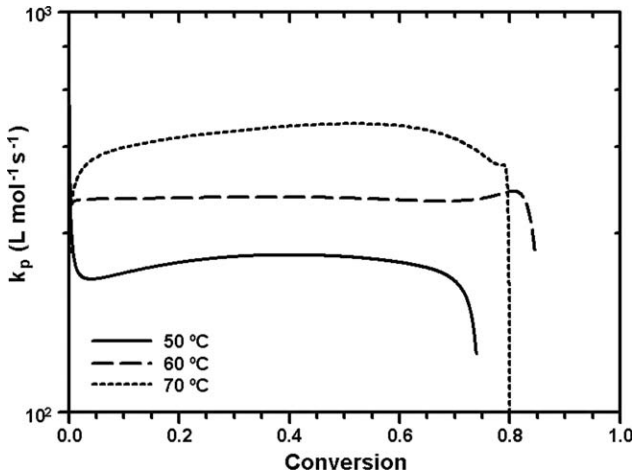

Figure 2. Propagation rate "constant" versus conversion at 50, 60, and 70 °C.

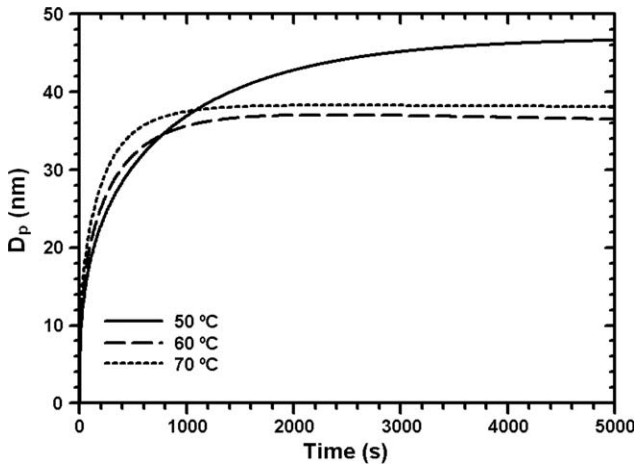

Figure 3. Particle diameter time evolution at 50, 60, and 70 °C.

Particle Diameter

The particle diameter evolution predictions with time are shown in Figure 3. The final particle diameter is in agreement with experimental data at T = [50, 60, 70]°C and D_p = [52.8, 46.2, 38.1] nm.[24] Here, the particle size decreases as the reaction temperature rises. The reason for having smaller particles as temperature increases, is due to higher entry to micelles (ρ_m) coefficients' values, resulting in a larger particle number N_T (= $N_0 + N_1$), as seen by adding eqs. (3) and (4) and by inspecting eq. (9). In addition, as depicted in eq. (10), the higher the reaction rates, the larger the active particle number. This is confirmed in Figure 1(b), comparing the inferred values against the model values. Two closely related facts occur and explain this result: (i) the reaction rate, which is proportional to the active particle concentration, increases with temperature; (ii) as a knock-on effect, micelles should feed monomer and surfactant to a larger number of active particles to preserve thermodynamic equilibrium. Then, the active particles do not swell as much as they would at relatively low temperatures, producing smaller particles. Summarizing, the model predicted a particle diameter decrease with increasing temperature, concurring with experimental and previously calculated data.[3,4,7,24]

Estimated Kinetic Parameters

The estimated parameters are listed in Table II, where the estimated parameters' values increase as temperature rises. In this table the overall coefficient of determination R^2 value is reported when fitting the experimental (x) and inferred (N_1) data. In the three runs, the obtained value is very close to one (R^2= 0.9999). Also, the standard deviation (σ) is very small for all the estimated parameters, being <3% (except in the case of k and k_o at 50°C, being around 14%) indicating an excellent level of certainty for all the values of the estimated parameters. The results corroborate former reaction schemes obtained before,[3,4] as follows: (i) the only event generating particles is radical entry to micelles (ρ_m). Homogeneous nucleation was taken into account with negligible contributions to particle production, given the low monomer water-solubility[11]; (ii) there is mass transfer from micelles to growing active particles (k_o) (approximated here by a coagulation mechanism between particles and micelles) and (iii) polymerization inside the particles ends with radical desorption (k) (preceded by the transfer to monomer event), rendering a dead polymer particle, agreeing with other works,[5–12] (iv) the radical entry to particles (ρ) and coagulation (k_c) between particles mechanisms can be disregarded, in accordance with our previous works,[3,4] given that their associated rate coefficients are ~12 orders of magnitude smaller, relative to those in (i), (ii), and (iii), which rule MEP kinetics.

Molar Mass

Chern and Wu reported the weight-average molar mass for the studied systems T = [50, 60, 70]°C and M_w = [8.4, 8.1, 7.48] × 10^5.[24] Here, a chain transfer constant estimation C_M (= $k_p/k_{tr,M}$) was obtained (Table II), fitting the reported values for the weight-average molar mass $\bar{M}_w$ with the values obtained solving eq. (7).[24] It was assumed that $\bar{M}_w$ is approximately equal to $2\bar{M}_n$. The determined chain transfer constant (C_M) value, about 2.4 × 10^{-4}, increased slightly with temperature. As a validation, the estimations reported before (see beginning of paragraph) are somewhat higher than the reported values of 0.6 − 0.92 × 10^{-4} and 0.45 × 10^{-4} for radical STY polymerization.[32,35] The weight-average molar mass calculation included the chain transfer-to-monomer and further radical desorption from the particle to the aqueous phase as termination events.

Arrhenius Dependency and Mechanisms Rates

Figure 4, with the resulting prefactor (A) and activation energy (E) listed in Table III, shows the Arrhenius dependency for all the estimated parameters, including its statistical report. It is worth highlighting that the parameters follow this function. Notably, Chern and Wu reported the radical desorption coefficient activation energy (15.3 kcal mol^{-1}),[24] which matches with the value obtained in this work (15.4 kcal mol^{-1}) almost perfectly. This result validates the present approach, given the

Table II. Fitted Parameters for Styrene MEP at 50, 60, and 70°C (N_{m0} = 3.51 × 10^{21} L^{-1})

T (°C)	$\rho_m \pm\sigma$ (s^{-1})	$k \pm\sigma$ (s^{-1})	$k_o \pm\sigma$ (L mol^{-1} s^{-1})	k_c (L mol^{-1} s^{-1})	ρ (s^{-1})	C_M	R^2	Overall standard deviation (σ_o)
T = 50°C	1.36 × 10^{-7} ± 5.87 × 10^{-11}	5.56 × 10^{-4} ± 7.78 × 10^{-5}	1421.19 ± 205.95	~0	~0	2.46 × 10^{-4}	0.99994	2.86 × 10^{-3}
T = 60°C	7.28 × 10^{-7} ± 7.13 × 10^{-11}	1.64 × 10^{-3} ± 1.98 × 10^{-6}	1957.15 ± 1.94	~0	~0	2.54 × 10^{-4}	0.99999	5.11 × 10^{-4}
T = 70°C	2.06 × 10^{-6} ± 2.02 × 10^{-9}	2.23 × 10^{-3} ± 2.00 × 10^{-5}	5172.90 ± 55.94	~0	~0	2.75 × 10^{-4}	0.99993	4.41 × 10^{-3}

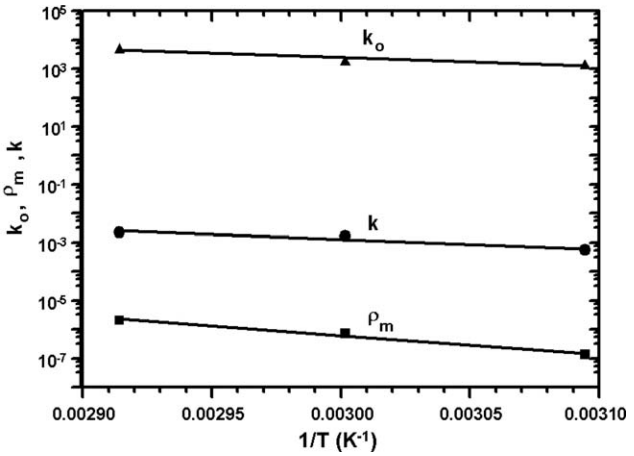

Figure 4. Rate parameters [$k(s^{-1})$, $\rho_m(s^{-1})$, and k_o (L mol^{-1} s^{-1})] against inverse temperature.

evident differences between the model given by Chern and Wu[24] and the one proposed in this work, mainly reflected in the non-linearity of N_1 evolution with reaction time and the lack of particle coagulation. Moreover, the activation energies for the other two events occurring in these MEP systems, k_o (monomer and surfactant transport) and ρ_m (radical entry to micelles), are reported for the first time.

E contains information regarding the energy needed for an event to occur. Following this reasoning, the smaller the E, the easier it is for the corresponding event to take place. It can be seen that k_o yields the smallest E and ρ_m the largest (Table III). Consistently, the monomer transfer from micelles to particles is the event with the largest rates. Analysis on the Arrhenius pre-factor is not straightforward, since the units of the constants differ given their nature (first order for k and ρ_m; and second order for k_o). Therefore, one should look at the rates associated with each event, thus sharing common framework. This comparison is plotted in Figure 5, where the ordinate axis has the reaction rate magnitude. It is clearly shown that the fastest event is the one associated with monomer transfer from micelles to particles, whose maximum value consistently occurred for the polymerization at 70°C. Meanwhile, the other two events (micellar nucleation and rate of radical desorption) show approximately the same rate range, making it difficult to discern which one is the fastest.

The curves depicting radical desorption [Figure 5(b)] and monomer-transfer from micelles to particles [Figure 5(c)] events show a complex evolution with time, starting from zero rate values and showing a maximum at early reaction stages. Thus,

Table III. Obtained Arrhenius Parameters for the Rate Constants Describing MEP

Parameter	A	E (cal mol^{-1})	σ	R^2
ρ_m (s^{-1})	2.92×10^{13}	30,004	±1.25	0.99992
k (s^{-1})	1.59×10^{7}	15,383	±1.35	0.99934
k_o (L mol^{-1} s^{-1})	4.77×10^{12}	14,156	±1.33	0.99999

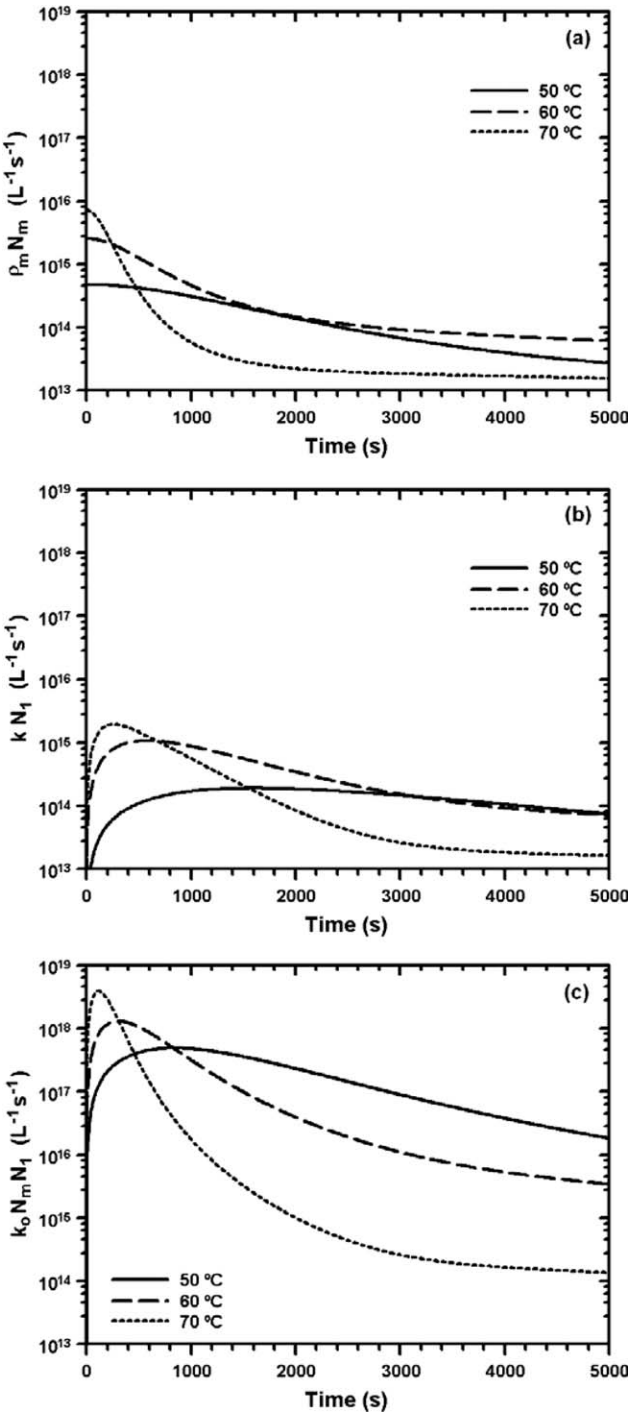

Figure 5. From top to bottom, rates of (a) nucleation by radical entry to micelles, (b) radical desorption from particles, and (c) monomer transfer from micelles to particles events as a function of time.

as the reaction temperature is increased, higher values are reached at longer times. In contrast, the evolution of the entry to micelles [Figure 4(a)] shows an initial decrease from the value dictated by the product $\rho_m N_{m0}$, being steeper as the reaction temperature is increased, and tending towards a steady state at high conversions.

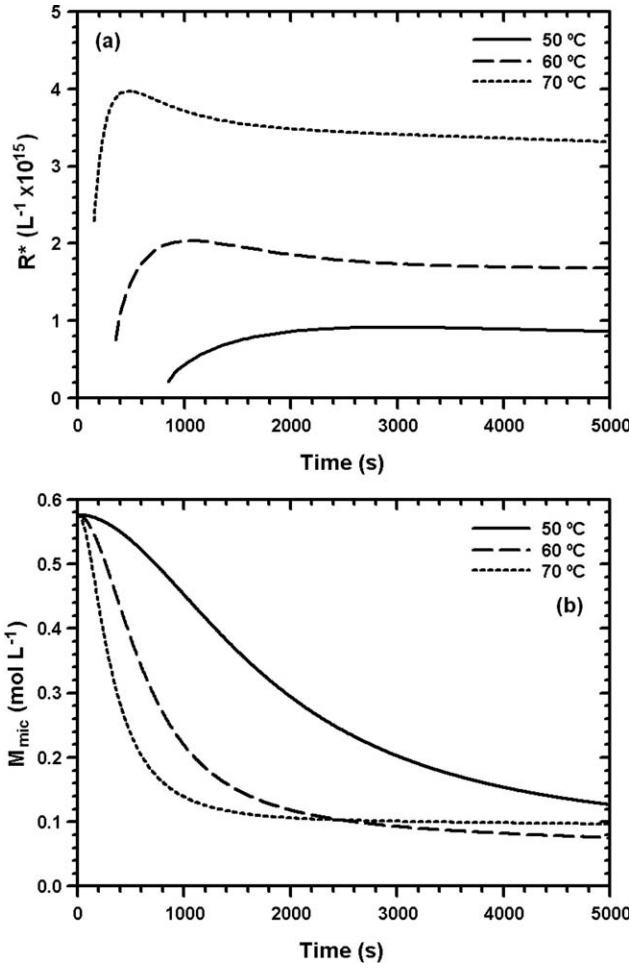

Figure 6. Model description for (a) Radical concentration in the water phase (R^*) and (b) monomer concentration in the micelles as a function of reaction time.

Aqueous-Phase Radical Concentration

The aqueous-phase radical concentration (R^*) and monomer content in the micelles (M_{mic}) were evaluated with the parameters obtained in this work. Figure 6 shows the evolution of these two quantities during the reaction. The radical concentration R^* [Figure 6(a)] increases sharply at early reaction times, showing an overshoot for data curves at 60 and 70°C, and reaching its steady-state value afterwards. Differently, the R^* curve at 50°C evolves monotonically and reaches its steady state. The monomer in the micelles, in turn, was consumed faster, the higher the reaction temperature, reaching a limit at which there is no further monomer consumption [Figure 6(b)]. This effect is more evident for the two higher temperatures, evidenced by a plateau in the corresponding curves. Thus, there is always a small amount of monomer remaining in all cases, evidencing no full conversion, regardless of the reaction conditions.

Parameters' Sensitivity Analysis

A sensitivity analysis was performed over several of the model parameters (not shown), specifically on C_{m0}, ρ, ρ_m, k, k_c, and k_o, by altering one order of magnitude their value as listed in Tables I and II, keeping the remaining parameters constant. The most important result is the confirmation that ρ_m, k, and k_o are the determining events in MEP kinetics for the systems considered, since they have the most outstanding effects on reaction kinetics.

When ρ_m grows, the polymerization rate increases sharply. The maxima defining the shape of the N_1 curves are shifted toward the beginning of the reaction, as any event promoting the reaction rate would do. The particle diameter (D_p) decreases and monomer in micelles is consumed sooner. The radical concentration in the aqueous phase (R^*) is sensitive to ρ_m variation as well, displaying sharper transients as ρ_m increases, but always reaching the same steady state at each temperature.

However, increasing the value of k renders lower conversions, N_1, D_p and more monomer in particles, as expected. As k_o is increased, lower conversions and smaller particle diameters are obtained, confirming that the micelles act as monomer reservoirs. Meanwhile, when k_o is decreased, the conversion trends are shifted to almost complete conversion, shedding light on the fact that the conversion is greatly favored by the particle production through radical entry to micelles.

Two quantities, which are very difficult to measure, and which influence the characteristics of the reaction and polymer in MEP, are the initial micellar concentration (N_{m0}) and the initial monomer concentration in the particles (C_{m0}). The first should be well established, since the rate of particle generation is strongly affected by the variation of ρ_m; that is, when N_{m0} is increased by one order of magnitude, ρ_m shrinks by an order of magnitude and vice versa. The C_{m0} value strongly affects the rate of polymerization and particle diameter, increasing them dramatically when the former is augmented.

Not surprisingly, it was found that k_c and ρ do not have any influence on the model predictions and that the variation in reaction temperature is not a factor triggering their presence in the MEP process. In accordance with previous studies,[3,4] we can firmly conclude that there is no particle coagulation and no radical entry to particles events in the MEP, in the studied systems. The last concluding result regarding the parametric study described above is that for the systems studied in a previous work for hexyl methacrylate (C_6MA), butyl methacrylate (nC_4MA) and STY, all using dodecyltrimethylammonium bromide (DTAB)/2-2′-azobis(2-amidinopropane) hydrochloride (V-50)/H_2O, they all follow the same patterns outlined in previous pages.[3,4]

CONCLUSIONS

The kinetic model presented here allowed its assessment, recognizing the main events occurring in MEP, and comparing them with the findings of other authors. The ID approach was successfully applied to the styrene batch MEP, at three different temperatures, aiding the inference of additional experimental data and further validating the 0-1 assumption. This proposal made possible a deeper insight into this polymerization mechanism. Furthermore, the Arrhenius parameters appearing in the kinetic events were obtained, validating their temperature dependence.

The E value for k is in accordance with the independently determined value reported by Chern and Wu. The model accurately

predicted the S-shaped conversion in the whole reaction time range and the bell-shaped active particle concentration evolution with time. It was confirmed that the active particle concentration (N_1) does not follow a linear behavior with time. The model slightly over-predicted the active particle concentration at the end of the reaction, with larger deviations at the lowest reaction temperature. This result was due to a diffusive effect in the reaction loci and explained by an abrupt k_p decrease at high conversions. The model predicted a particle diameter decrease with increasing temperature, concurring with experimental and previously calculated data. It was confirmed that the radical entry to particles (ρ) and coagulation (k_c) events can be neglected, agreeing with some reports and disagreeing with others, showing that the reaction temperature variations do not trigger these events. Applying a sensitivity analysis to the proposed model predictions supported the confirmation that ρ_m, k and k_o rule the MEP for the analyzed systems, the monomer transfer to particles from micelles–characterized by k_o–being the fastest. Besides, this analysis revealed that the increase in reaction rate (by varying the coefficients or raising the temperature) had an interesting effect on the position of the maxima defining the bell-shaped form of N_1: the faster the reaction, the earlier the appearance of this maximum in N_1 during the polymerization. In general, the aqueous phase radical concentration increased as temperature raised, and remained nearly constant throughout the reaction, validating our original steady-state assumption.

ACKNOWLEDGMENTS

Funds were provided by UNAM (PAPIIT IN211215), including a scholarship for one of the participants (JELA). The authors also thank Ms. Kathryn L. Erickson for reviewing the English in this article.

REFERENCES

1. Mendizábal, E.; Flores, J.; Puig, J. E.; López-Serrano, F.; Álvarez, J. *Eur. Polym. J.* **1998**, *34*, 411.
2. Mendizábal, E.; Flores, J.; Puig, J. E.; Katime, I.; López-Serrano, F.; Álvarez, J. *Macromol. Chem. Phys.* **2000**, *201*, 1259.
3. López-Serrano, F.; López-Aguilar, J. E.; Mendizábal, E.; Puig, J. E.; Álvarez, J. *Ind. Eng. Chem. Res.* **2008**, *47*, 5924.
4. López-Serrano, F.; López-Aguilar, J. E.; Mendizábal, E.; Puig, J. E.; Álvarez, J. *Macromol. Symp.* **2008**, *271*, 94.
5. Guo, J. S.; Sudol, E. D.; Vanderhoff, J. W.; El-Aasser, M. S. *J. Polym. Sci. Part A: Polym. Chem.* **1992**, *30*, 691.
6. Guo, J. S.; Sudol, E. D.; Vanderhoff, J. W.; El-Aasser, M. S. *J. Polym. Sci. Part A: Polym. Chem.* **1992**, *30*, 703.
7. Nomura, M.; Suzuki, K. *Macromol. Chem. Phys.* **1997**, *198*, 3025.
8. Nomura, M.; Suzuki, K. *Ind. Eng. Chem. Res.* **2005**, *44*, 2561.
9. Suzuki, K.; Nomura, M.; Harada, M. *Colloid Surf. A* **1999**, *153*, 23.
10. Morgan, J. D.; Lusvardi, K. M.; Kaler, E. W. *Macromolecules* **1997**, *30*, 1897.
11. de Vries, R.; Co, C. C.; Kaler, E. W. *Macromolecules* **2001**, *34*, 3233.
12. Co, C. C.; de Vries, R.; Kaler, E. W. *Macromolecules* **2001**, *10*, 3224.
13. Chern, C. S.; Tang, H. J. *J. Appl. Polym. Sci.* **2005**, *97*, 2005.
14. López-Serrano, F.; Mendizábal, E.; Puig, J. E.; Álvarez, J. *Macromol. Symp.* **2009**, *283-284*, 18.
15. López-Serrano, F.; Fernández, C. R.; Puig, J. E.; Alvarez, J. *Macromol. Symp.* **2000**, *150*, 59.
16. López-Serrano, F.; Puig, J. E.; Alvarez, J. *AIChE J.* **2004**, *50*, 2246.
17. López-Serrano, F.; Puig, J. E. *Ind. Eng. Chem. Res.* **2004**, *43*, 7361.
18. López-Serrano, F.; Puig, J. E.; Alvarez, J. *Ind. Eng. Chem. Res.* **2007**, *46*, 2455.
19. Puig, J. E.; Mendizábal, E.; López-Serrano, F.; López, R. G. In Encyclopedia of Surface and Colloid Science, 2nd ed.; Somasundaram, P., Ed.; Taylor & Francis: London, **2012**, DOI: 10. 1081/E-ESCS-20047408.
20. He, H.; Pan, Q.; Rempel, G. L. *J. Appl. Polym. Sci.* **2007**, *105*, 2129.
21. He, H.; Pan, Q.; Rempel, G. L. *Ind. Eng. Chem. Res.* **2007**, *46*, 1682.
22. O'Donnell, J. M.; Kaler, E. W. *J. Polym. Sci. Part A: Polym. Chem.* **2010**, *48*, 604.
23. O'Donnell, J. M. *Chem. Soc. Rev.* **2012**, *41*, 3061.
24. Chern, C. S.; Wu, L. J. *J. Polym. Sci. Part A: Polym. Chem.* **2001**, *39*, 3199.
25. Full, A. P.; Kaler, E. W.; Arellano, J.; Puig, J. E. *Macromolecules* **1996**, *29*, 2764.
26. Buback, M.; Gilbert, R. G.; Hutchinson, R. A.; Klumperman, B.; Kuchta, F. D.; Manders, B.; O'Driscoll, K. F.; Russell, G. T.; Schweer, J. *Macromol Chem Phys.* **1995**, *196*, 3267.
27. Buback, M.; Kuchta, F. D. *Macromol. Chem. Phys.* **1997**, *198*, 1455.
28. Staicu, T.; Micutz, M.; Cristescu, G.; Leca, M. *Rev. Roum. Chim.* **2008**, *53*, 481.
29. Schrader, D. In Polymer Handbook, 4th ed.; Brandrup, J., Immergut, E. H., Grulke, E. A. Eds.; Wiley, New York: **1999** ISBN 0471166286.
30. Santos, A. F.; Lima, E. L.; Pinto, J. C.; Graillat, C.; McKenna, T. *J. Appl. Polym. Sci.* **2003**, *90*, 1213.
31. Gilbert, R. G. Emulsion Polymerization: Mechanistic Approach; Academic PressLondon, United Kingdom, **1995**.
32. Odian, G. Principles of Polymerization; WileyNew Jersey, USA, **2004**.
33. Conte, S. D.; De Boor, C. Elementary Numerical Analysis: Algorithmic Approach; Springer: McGraw-Hill: New York, **1980**.
34. Fogler, H. S. Elements of Chemical Reaction Engineering: Prentice-Hall: New York, **2005**.
35. Co, C. C.; Cotts, P.; Burauer, S.; de Vries, R.; Kaler, E. W. *Macromolecules* **2001**, *34*, 3245.